



Modelling the Impact of Decomposed Disease-Induced Dead Cashew Plants on Fusarium Wilt Dynamics in South-Eastern Tanzania

Fatu Chilinga^{1,*} & Alfred K. Hugo¹

¹Department of Mathematics and Statistics, The University of Dodoma, P.O. Box 338, Dodoma, Tanzania

*E-mail: fchilinga@yahoo.com

Abstract. Cashew Fusarium wilt disease transmitted by *Fusarium oxysporum* is dangerous and destroys many cashew plants in Tanzania. The effect of this disease leads households and the government to experience a decrease in overall cashew production and income due to this disease's capacity to harm cashew plants. This study aimed to ascertain the role of Fusarium wilt-decayed disease-induced dead plants in spreading the disease among cashew plants. A mathematical model was created based on the dynamics of the disease and a stability analysis was conducted using theories of ordinary differential equations. Data from two regions in Tanzania, Lindi, and Mtwara, were used in model fitting and parameter estimation. Additionally, the parameters were estimated using maximum likelihood estimation (MLE). The outcome suggests that the disease's prevalence and spread increase during an outbreak as decomposed diseased-induced dead plants contribute to the saturation of chlamydospores in the soil.

Keywords: *cashew plants; Fusarium wilt; Fusarium oxysporum; disease-induced death; parameter estimation.*

1 Introduction

The consumption of cashew nuts in the world market is growing yearly because of their widely appreciated taste and high nutrient content [1]-[3]. Frequent consumption of cashew nuts minimizes cholesterol, hypertension, coronary heart disease, and diabetes [4],[5]. Furthermore, the cashew nut is a cash product in most countries where it is grown, increasing the foreign exchange earnings for the nation and as a source of income for most families [6].

The cashew nut is cultivated worldwide. Africa contributes about 40% of worldwide production, while Tanzania generates roughly 20% of all African production [7]. More than 80% of the total output in Tanzania comes from the Lindi and Mtwara regions [8]. Cashew nuts are the main cash crop for many families in the southern regions and contribute up to 10% of the total value of earnings in foreign currencies [9].

Received September 22nd, 2022, Revised June 1st, 2023, Accepted for publication July 4th, 2023

Copyright © 2023 Published by ITB Institute for Research and Community Service, ISSN: 2337-5760,

DOI: 10.5614/j.math.fund.sci.2023.55.1.3

Despite the significant contribution to the nation and the continent, cashew nut production has been impacted by numerous issues, such as diseases, declining soil fertility, drought, and insect pests [10],[11]. Cashew Fusarium wilt disease destroys many cashew plants in Tanzania, which is where the disease was first discovered [12]. The disease is caused by a soil-borne fungus called *Fusarium oxysporum* [12]-[14]. As a result of this disease's ability to damage cashew plants, households and the nation's overall cashew production and income are reduced [12],[15].

Fusarium wilt disease outbreaks have been experienced in the south-eastern part of Tanzania, including the Mtwara Rural, Newala, Masasi and Tandahimba districts in the Mtwara region and Liwale, Nachingwea and Ruangwa districts in the Lindi region [15]. The main transmission of Fusarium wilt disease is through root contact [16]. Dead infected cashew plants contribute to disease transmission [17]. The fungus in diseased-induced dead cashew plants invades the plant tissue and produces macroconidia. After the host tissue has degraded, chlamydospores are produced and end up in the soil when the tissue collapses [18]. This is possible when disease-induced dead plants are left to decompose in the field. Farmers usually leave the dead plants to deteriorate in the field, as indicated in Figure 1.



Figure 1 Photograph of disease-induced dead cashew plant. Source: Field data, 2020.

Mathematical modelling is essential for understanding disease dynamics and suggesting appropriate control methods for minimizing infectious diseases [19]-[24]. Plant disease dynamics can be modelled mathematically, as has been shown in different studies. For example, Burie *et al.* [25] investigated vineyard fungal disease through a mathematical model and devised short and long-term solutions. Anggriani [26] analyzed plant-fungal epidemics and ended up with remedial

factors against infection. Nisar *et al.* [27] modelled the Gemini virus in capsicum annum and developed the best strategy for eliminating the disease at an affordable cost.

Additionally, mathematical modelling assists decision-makers in deciding on the most effective control strategies by using the information from a sensitivity analysis that identifies the parameters that contribute to the spread of the disease [28]-[32].

This study applied mathematical theories in modelling the role of decomposed disease-induced dead cashew plants in disease transmission and persistence during an outbreak. The findings can help to develop strategies for disease management and understanding how the disease develops and spreads over time.

2 Model Formulation

This section deals with the model formulation whereby cashew plants are divided into five subpopulations. The susceptible plant (P) is a cashew plant that is disease-free yet prone to infection when the fungus comes into contact with it. The plants become exposed (E) after touching diseased plants or contaminated soil through its wounds or roots [14],[33]-[36]. After two to six months, the exposed population becomes infectious (W). The infectious population can either be treated and join the treated population (T) or die due to disease and join the dead class (D) [15]. Also, there are two subgroups of the fungal population, i.e., macroconidia spores (M) and chlamydospores (H). Macroconidia spores occur on the exterior of disease-induced dead plants. Macroconidia spores on the surface of disease-induced dead plants produce chlamydospores and fall to the ground [13],[37].

The model was developed assuming that the population growth of cashew plants follows a logistic behavior, where r is the growth rate and k_1 is the carrying capacity. The contact rate between fungus and plants is modelled by β with the infection rate expressed as follows:

$$\beta = \left(\frac{\tau_1 H}{d + H} + \tau_2 W \right). \quad (1)$$

The parameter τ_1 represents the contact rate between vulnerable cashew plants and chlamydospores, while τ_2 is the contact rate between susceptible cashew

plants and diseased plants [14]. The parameter d denotes the ground-level chlamydospore saturation constant rate. The parameter ω represents the progression rate of the exposed population to the infected population within two to six months [18]. Cashew plants that are not seriously infected may regain health after treatment at rate ρ and develop susceptibility with rate ϕ [15]. Cashew plants that are more seriously impacted have a lower survival rate and perish at a rate of θ , or die naturally at a rate of α [15]. Usually, farmers remove some dead plants from the field for other uses while some dead plants remain to decompose in the field, denoted by ν . Microconidia spores attack the tissue of dying plants to produce macroconidia spores from the sporodochia [37]-[42]. The parameter ψ defines the rate at which exposed, infected, and disease-induced dead plants produce macroconidia spores. The following equation represents this parameter:

$$\psi = \nu E + \gamma W + \pi D. \quad (2)$$

Macroconidia produce chlamydospores at rate η [43]-[45]. Chlamydospores are thick-walled, which helps them to survive in an unfavorable environment for a long time [46]. Chlamydospores leave the living class due to deterioration at rate μ [13].

2.1 Parameter Descriptions

Based on the description of the dynamics of Fusarium wilt disease and the assumptions, the compartmental diagram in Figure 2 captures the constructed interaction between cashew plants and Fusarium oxysporum fungus.

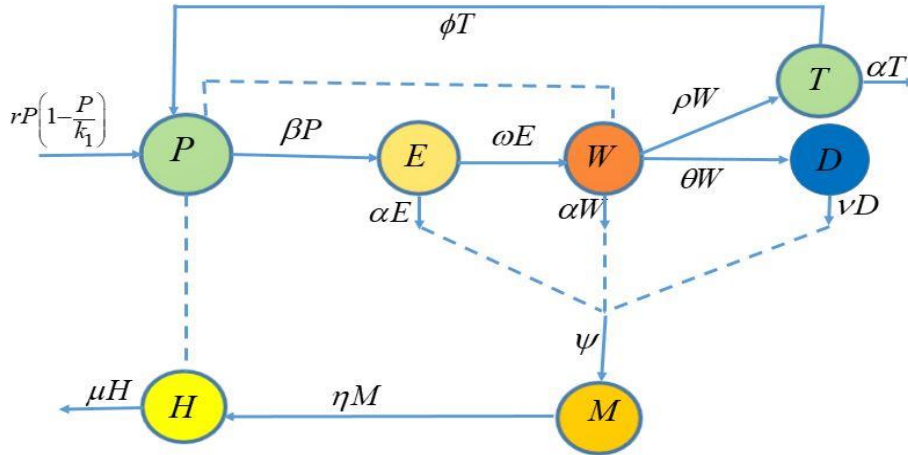


Figure 2 Compartment flow diagram.

The model parameters used are summarized in Table 1.

Table 1 Parameters and their description for Fusarium wilt disease

Symbol	Description
r	Cashew plant's growth rate
τ_1	Contact rate between susceptible cashew plants and chlamydospores
τ_2	Contact rate between susceptible and infected cashew plants
k_1	Carrying capacity of cashew plants
d	Chlamydospores saturation in the soil
ω	Rate of progression from exposed population to infected population
α	Rate of natural death
θ	Disease-related mortality rate
ν	Disease-induced dead plants left to decompose in the field
ϕ	Rate at which recovered plants return to the susceptible class
υ	Production rate of macroconidia from dead exposed plants
γ	Production rate of macroconidia from dead infected plants
π	Production rate of macroconidia from disease-induced dead plants
η	Production rate of chlamydospores
μ	Decay rate of chlamydospores

2.2 Mathematical Equations

Considering the flow diagram, we developed mathematical equations that show the transmission dynamics of the Fusarium wilt disease using the ordinary differential equation:

$$\begin{aligned}
 \frac{dP}{dt} &= rP \left(1 - \frac{P}{k_1} \right) + \phi T - \left(\frac{\tau_1 H}{d + H} + \tau_2 W \right) P \\
 \frac{dE}{dt} &= \left(\frac{\tau_1 H}{d + H} + \tau_2 W \right) P - (\alpha + \omega) E \\
 \frac{dW}{dt} &= \omega E - (\alpha + \rho + \theta) W \\
 \frac{dT}{dt} &= \rho W - (\alpha + \phi) T
 \end{aligned} \tag{3}$$

$$\begin{aligned}\frac{dD}{dt} &= \theta W - \nu D \\ \frac{dM}{dt} &= \nu E + \gamma W + \pi D - \eta M \\ \frac{dH}{dt} &= \eta M - \mu H\end{aligned}$$

3 Qualitative Analysis

A qualitative analysis of the model was conducted to gain insight into the dynamical characteristics of model (3) and to better comprehend the effects of the presence of decomposed plants.

3.1 Non-negativity of the Solution

It must be demonstrated that all system solutions with positive initial values remain positive for model system (3) to be epidemiologically significant and adequately posed. The following theorem will prove this.

Theorem 3.1

Assume that $P(0) > 0$, $E(0) > 0$, $W(0) > 0$, $T(0) > 0$, $D(0) > 0$, $M(0) > 0$ and $H(0) > 0$. Then, the solutions $P(t)$, $E(t)$, $W(t)$, $T(t)$, $D(t)$, $M(t)$, $H(t)$ of model (3) are positive $\forall t > 0$.

Proof. Consider the first equation in model (3) that forms the following inequality:

$$\frac{dP(t)}{P(t)} \geq - \left(\frac{\tau_2 H(t)}{d + H(t)} + \tau_1 W(t) \right) dt .$$

Solving for t and $P(t) = P(0)$, we get:

$$P(t) \geq P(0) e^{- \int_0^t \left(\frac{\tau_2 H(t)}{d + H(t)} + \tau_1 W(t) \right) dt} .$$

As $t \rightarrow \infty$, the value of $P(t) \geq P(0) e^{- \int_0^t \left(\frac{\tau_2 H(t)}{d + H(t)} + \tau_1 W(t) \right) dt} \geq 0$, since

$$\frac{\tau_2 H(t)}{d + H(t)} + \tau_1 W(t) \geq 0.$$

A similar proof can be established for the remaining equation in the \mathfrak{R}_+^7 region and the system can be used to research cashew disease since it is meaningful.

3.2 Existence and Uniqueness of the Solution

Considering the general form of ordinary first-order differential equations,

$$\frac{dy}{dt} = f(t, y) \quad (4)$$

where the initial value t_0 with respect to the function can be written as $y(t_0) = y_0$.

The following theorem shows the existence of a unique solution of the Fusarium wilt disease model.

Theorem 3. 2

Assume there exists a domain D such that:

$$|t - t_0| \leq p, |y - y_0| \leq q, \quad (5)$$

and if $g(t, y)$ satisfies the Lipschitz condition such that:

$$\|G(t, y_1) - G(t, y_2)\| \leq b \|y_1 - y_2\| \quad (6)$$

where G is a function and at any time point $(t, y_1) \in D$ and $(t, y_2) \in D$, the parameter b represents a positive constant. Then, there is a constant $\varepsilon > 0$ such that \exists is a continuous solution $y(t)$ of system (1) such that $|t - t_0| \leq \varepsilon$. The system should also satisfy the following condition:

$$\frac{\partial G_i}{\partial y_j}, i, j = 1, 2, 3, \dots, n \quad (7)$$

It is bounded and continuous within the domain D .

Lemma 3.1 If $G(t, y)$ is a continuous partial derivative $\frac{\partial G_i}{\partial y_j}$ on a bounded and closed convex domain D that satisfies the Lipschitz condition. Hence, we need to find a fixed solution to the following form:

$$0 < D < \infty \quad (8)$$

Theorem 3.3 Assume that the domain D satisfies conditions (6) and (7) in theorem 3.2. Then a mathematical solution to model (3) is bounded in domain D .

Proof. The proof of theorem 3.3 is obtained by considering lemma 3.1. Consider the following equations:

$$\begin{aligned} G_1 &= rP \left(1 - \frac{P}{k_1} \right) + \phi T - \left(\frac{\tau_1 H}{d + H} + \tau_2 W \right) P \\ G_2 &= \left(\frac{\tau_1 H}{d + H} + \tau_2 W \right) P - (\alpha + \omega) E \\ G_3 &= \omega E - (\alpha + \rho + \theta) W \\ G_4 &= \rho W - (\alpha + \phi) T \\ G_5 &= \theta W - \nu D \\ G_6 &= \nu E + \gamma W + \pi D - \eta M \\ G_7 &= \eta M - \mu H \end{aligned} \quad (9)$$

We need to show that $\frac{\partial G_i}{\partial y_j}, j = 1, 2, \dots, 7$ are bounded and continuous. The

following are the partial derivatives of model (9) for a unique equation. Considering the first equation in model (9), we have:

$$G_1 = rP \left(1 - \frac{P}{k_1} \right) + \phi T - \left(\frac{\tau_1 H}{d + H} + \tau_2 W \right) P.$$

The partial derivative of function G_1 with respect to class P is:

$$\frac{\partial G_1}{\partial P} = r \left(1 - \frac{P}{k_1} \right) - \frac{\tau_1 H}{d + H} - \tau_2 W.$$

Take the absolute value of both sides by considering condition (8), we get:

$$\left| \frac{\partial G_1}{\partial P} \right| = \left| r \left(1 - \frac{P}{k_1} \right) - \frac{\tau_1 H}{d + H} - \tau_2 W \right| < \infty.$$

Then finding the partial derivative of function G_1 with respect to class W gives:

$$\frac{\partial G_1}{\partial W} = -\tau_2 P \text{ thus } \left| \frac{\partial G_1}{\partial W} \right| = |-\tau_2 P| < \infty.$$

Also, the partial derivative of function G_1 with respect to class T gives:

$$\frac{\partial G_1}{\partial T} = \varphi, \text{ then } \left| \frac{\partial G_1}{\partial T} \right| = |\varphi| < \infty.$$

Lastly, find the partial derivative of function G_1 with respect to class H gives:

$$\frac{\partial G_1}{\partial H} = -S \left(-\frac{\tau_1 H}{(d + H)^2} + \frac{\tau_1}{d + H} \right).$$

With condition (6), we have:

$$\left| \frac{\partial G_1}{\partial H} \right| = \left| -P \left(-\frac{\tau_1 H}{(d + H)^2} + \frac{\tau_1}{d + H} \right) \right| < \infty.$$

Then, consider the second equation in model system (8). We have:

$$G_2 = \left(\frac{\tau_1 H}{d + H} + \tau_2 W \right) P - (\alpha + \omega) E.$$

Its partial derivative with respect to class P is as follows:

$$\frac{\partial G_2}{\partial P} = \frac{\tau_1 H}{d + H} + \tau_2 W, \text{ thus } \left| \frac{\partial G_2}{\partial P} \right| = \left| \frac{\tau_1 H}{d + H} + \tau_2 W \right| < \infty.$$

The partial derivative of function G_2 with respect to class E is as follows:

$$\frac{\partial G_2}{\partial E} = -\alpha - \omega.$$

By considering condition (7), we get:

$$\left| \frac{\partial G_2}{\partial E} \right| = |-\alpha - \omega| < \infty.$$

Again, the partial derivative of function G_2 with respect to class W is as follows:

$$\frac{\partial G_2}{\partial W} = \tau_2 P$$

Taking the absolute value, we get:

$$\left| \frac{\partial G_2}{\partial W} \right| = |\tau_2 P| < \infty.$$

The remaining equations in model system (9) should be solved using a similar methodology. This demonstrates that every partial derivative is continuous and bounded. Hence, this proves the existence and uniqueness of the solution of system (3) in region D .

3.3 Fusarium Wilt Equilibria

The Fusarium wilt disease-free equilibrium point (E_0) is given by:

$$E_0 = (k_1, 0, 0, 0, 0, 0, 0)$$

And the endemic equilibrium points (E_*) are:

$$P^* = \frac{\alpha(\alpha + \omega)W^*}{\left(\frac{\tau_1}{d} + \tau_2 W^*\right)\omega}, \quad E^* = \frac{\alpha W^*}{\omega}, \quad T^* = \frac{\rho W^*}{\alpha + \phi}, \quad D^* = \frac{\theta W^*}{\nu}, \quad H^* = \frac{\eta M^*}{\mu}$$

and $M^* = \frac{\left(\gamma + \frac{\pi\theta}{\nu} + \frac{\alpha\nu}{\omega}\right)}{\eta} W^*.$

3.4 Reproduction Number Analysis

The basic reproduction number \mathfrak{R}_0 was used to investigate the local and global stability of model system (3). The calculation of \mathfrak{R}_0 was done by using the next-generation operation method in [47].

$$F = \begin{bmatrix} \left(\frac{\tau_1 H}{d+H} + \tau_2 W \right) P \\ 0 \\ 0 \\ 0 \\ 0 \end{bmatrix} \text{ and } V = \begin{bmatrix} (\alpha + \omega) E \\ \omega E - (\alpha + \rho + \theta) W \\ \theta W - \nu D \\ \nu E + \gamma W + \pi D - \eta M \\ \eta M - \mu H \end{bmatrix} \quad (10)$$

Assume matrix $F(x)$ is the Jacobian matrix from F and $V(x)$ is the Jacobian matrix from V . The matrices $F(x)$ and $V(x)$ at disease-free equilibrium $E_0 = (k_1, 0, 0, 0, 0, 0)$ obtained are:

$$F(x) = \begin{bmatrix} 0 & k_1 \tau_1 & 0 & 0 & k_1 \tau_2 \\ 0 & 0 & 0 & 0 & 0 \\ 0 & 0 & 0 & 0 & 0 \\ 0 & 0 & 0 & 0 & 0 \\ 0 & 0 & 0 & 0 & 0 \end{bmatrix} \quad (11)$$

$$V(x) = \begin{bmatrix} \alpha + \omega & 0 & 0 & 0 & 0 \\ -\omega & \alpha + \theta + \rho & 0 & 0 & 0 \\ 0 & -\theta & \nu & 0 & 0 \\ -\nu & -\gamma & -\pi & \eta & 0 \\ 0 & 0 & 0 & -\eta & \mu \end{bmatrix} \quad (12)$$

The next-generation matrix obtained is:

$$FV^{-1} = \begin{bmatrix} \frac{k_1 \omega \tau_1}{(\alpha + \theta + \rho)(\alpha + \omega)} + \frac{k_1 \tau_2 \eta (\nu \nu (\alpha + \theta + \rho) + \omega (\pi \theta + \gamma \nu))}{d \eta \mu \nu (\alpha + \theta + \rho)(\alpha + \omega)} & \frac{k_1 \tau_1 (\mu \nu \eta (\alpha + \omega))}{\eta \mu \nu (\alpha + \theta + \rho)(\alpha + \omega)} + \frac{k_1 \eta (\pi \theta + \gamma \nu)(\alpha + \omega)}{d \eta \mu \nu (\alpha + \theta + \rho)(\alpha + \omega)} & \frac{k_1 \tau_2 \pi}{d \mu \nu} & \frac{k_1 \tau_2}{d \mu} & \frac{k_1 \tau_2}{d \mu} \\ 0 & 0 & 0 & 0 & 0 \\ 0 & 0 & 0 & 0 & 0 \\ 0 & 0 & 0 & 0 & 0 \\ 0 & 0 & 0 & 0 & 0 \end{bmatrix} \quad (13)$$

$$|\lambda I - FV^{-1}| = \begin{bmatrix} \lambda - \frac{k_1 \omega \tau_1}{(\alpha + \theta + \rho)(\alpha + \omega)} - \frac{k_1 \tau_2 \eta (\nu \nu (\alpha + \theta + \rho) + \omega (\pi \theta + \gamma \nu))}{d \eta \mu \nu (\alpha + \theta + \rho)(\alpha + \omega)} & \frac{k_1 \tau_1 (\mu \nu \eta (\alpha + \omega))}{\eta \mu \nu (\alpha + \theta + \rho)(\alpha + \omega)} + \frac{k_1 \eta (\pi \theta + \gamma \nu)(\alpha + \omega)}{d \eta \mu \nu (\alpha + \theta + \rho)(\alpha + \omega)} & \frac{k_1 \tau_2 \pi}{d \mu \nu} & \frac{k_1 \tau_2}{d \mu} & \frac{k_1 \tau_2}{d \mu} \\ 0 & \lambda & 0 & 0 & 0 \\ 0 & 0 & \lambda & 0 & 0 \\ 0 & 0 & 0 & \lambda & 0 \\ 0 & 0 & 0 & 0 & \lambda \end{bmatrix} \quad (14)$$

The eigenvalues obtained are:

$$\lambda_1 = 0, \lambda_2 = 0, \lambda_3 = 0, \lambda_4 = 0, \lambda_5 = \frac{k_1 \omega \tau_1}{(\alpha + \theta + \rho)(\alpha + \omega)} + \frac{k_1 \tau_2 (\nu \nu (\alpha + \theta + \rho) + \omega (\pi \theta + \gamma \nu))}{d \mu \nu (\alpha + \theta + \rho)(\alpha + \omega)}$$

The reproductive number is the absolute largest eigenvalue obtained, which is:

$$\mathfrak{R}_0 = \frac{k_1 \omega \tau_1}{(\alpha + \theta + \rho)(\alpha + \omega)} + \frac{k_1 \tau_2 (\nu \nu (\alpha + \theta + \rho) + \omega (\pi \theta + \gamma \nu))}{d \mu \nu (\alpha + \theta + \rho)(\alpha + \omega)}. \quad (15)$$

The basic reproduction number represents the projected number of each plant infected by the initially diseased plants for their whole infectious period. It serves as a predictor of the ability of infectious and parasitic organisms to spread.

3.5 Local Stability

A stability study of the disease-free equilibrium point of model system (3) was conducted using the Routh-Hurwitz criterion [48]. Consider Theorem 3.4 below.

Theorem 3.4

The Fusarium wilt disease-free equilibrium point is locally asymptotically stable if and only if the major diagonal of the Jacobian matrix is positive.

Proof. Assume that each equation in the system is differentiated, considering its state variable at E_0 . The Jacobian matrix at E_0 is as follows:

$$J_{E_0} = \begin{bmatrix} -r & k_1 \tau_2 & 0 & \phi & 0 & 0 & \frac{-k_1 \tau_1}{d} \\ 0 & -(\alpha + \omega) & k_1 \tau_2 & 0 & 0 & 0 & \frac{k_1 \tau_1}{d} \\ 0 & \omega & -(\alpha + \theta + \rho) & 0 & 0 & 0 & 0 \\ 0 & 0 & \rho & -(\alpha + \phi) & 0 & 0 & 0 \\ 0 & 0 & \theta & 0 & -\nu & 0 & 0 \\ 0 & \nu & \gamma & 0 & \pi & -\eta & 0 \\ 0 & 0 & 0 & 0 & 0 & \eta & -\mu \end{bmatrix} \quad (16)$$

Computing the eigenvalues of the Jacobian matrix J_{E_0} , we obtain $-r$ and $-(\alpha + \phi)$. Then the remaining eigenvalues will be obtained from matrix H below.

$$H = [A_{ij}] = \begin{bmatrix} -(\alpha + \omega) & k_1 \tau_2 & 0 & 0 & \frac{k_1 \tau_1}{d} \\ \omega & -(\alpha + \theta + \rho) & 0 & 0 & 0 \\ 0 & \theta & -\nu & 0 & 0 \\ \nu & \gamma & \pi & -\eta & 0 \\ 0 & 0 & 0 & \eta & -\mu \end{bmatrix} \quad (17)$$

To obtain the remaining eigenvalues, we consider the polynomial roots $|H - \lambda| = 0$ that give the characteristic equation (18):

$$\lambda^5 + c_1 \lambda^4 + c_2 \lambda^3 + c_3 \lambda^2 + c_4 \lambda + c_5 = 0. \quad (18)$$

where:

$$\begin{aligned} c_1 &= \mu + \eta + \nu + 2\alpha + \theta + \rho + \omega \\ c_2 &= \alpha^2 + 2\alpha(\eta + \mu + \nu) + \alpha(\omega + \rho + \theta) + \eta(\mu + \nu) + \\ &\quad \omega(\mu + \nu + \omega + \rho + \theta) + \mu(\nu + \omega + \rho + \theta) + \nu(\omega + \rho) - \omega k_1 \tau_2 \\ c_3 &= \frac{1}{d} \left(d\alpha^2(\eta + \mu + \nu) + 2d\alpha\eta(\mu + \nu) + \alpha d\omega(\theta + \rho + \omega) + \right. \\ &\quad \left. \alpha d\mu(2\nu + \omega + \rho + \theta) + \alpha d\nu(\theta + \rho + \omega) + d\eta\mu(\theta + \rho + \omega) + \right. \\ &\quad \left. d\eta\nu(\theta + \rho + \omega) + d\eta\omega(\theta + \rho) + d\mu\nu(\theta + \rho + \omega) + d\mu\omega(\theta + \rho) \right. \\ &\quad \left. + d\nu\omega(\theta + \rho) - d\omega k_1 \tau_2(\eta + \mu + \nu) - \eta\nu k_1 \tau_1 \right) \\ c_4 &= \frac{1}{d} \left(\alpha^2 d(\eta\mu + \eta\nu + \mu\nu) + \alpha d\eta\mu(\omega + 2\nu + \rho + \theta) + \alpha d\eta\nu(\omega + \rho + \theta) \right. \\ &\quad \left. + \alpha d\mu(\omega + \rho + \theta) + d\eta\mu\nu(\omega + \rho + \theta) + d\eta\mu\omega(\rho + \theta) + \right. \\ &\quad \left. d\eta\nu\omega(\rho + \theta) + d\mu\nu\omega(\rho + \theta) + k_1 \tau_1 \eta(\nu\nu + \gamma\omega + \rho\nu + \theta\nu) - \right. \\ &\quad \left. k_1 \tau_2 d\omega(\eta\mu + \eta\nu + \nu\mu) - k_1 \tau_1 \alpha \eta \nu \right) \\ c_5 &= \frac{1}{d} \left(d\mu\nu\alpha(\alpha + \omega + \rho + \theta) + d\mu\nu\omega(\rho + \theta) + k_1 \tau_1 \nu(\gamma\omega + \rho\nu + \theta\nu) - \right. \\ &\quad \left. k_1 \tau_1 \alpha \nu \nu - k_1 \tau_2 \mu d\omega\nu + \pi\omega\theta k_1 \tau_1 + k_1 \tau_1 \nu(\gamma\omega + \rho\nu + \theta\nu) \right) \end{aligned}$$

The positivity of the principal leading diagonal of matrix H_n makes the disease-free equilibrium point locally stable. In light of this, the disease-free equilibrium point is only locally stable when $\Delta H_1, \Delta H_2, \dots, \Delta H_5 > 0$. Then, $\Delta H_1 > 0$ since we have

$$\mu + \eta + \nu + 2\alpha + \theta + \rho + \omega > 0$$

Then, for $\Delta H_2 > 0$, if and only if $c_1 c_2 > c_3$, $\Delta H_3 > 0$, if $c_1 c_2 c_3 + c_3^2 > c_1 c_4 + c_5$, $\Delta H_4 > 0$ if $c_1 c_2 c_3 c_4 + c_2 c_3 c_5 + c_5^2 > c_2 c_5 + c_1^2 c_4^2 + c_3^2 c_4^2$, and lastly $\Delta H_5 > 0$ if $c_1 c_2 c_3 c_4 c_5 + c_1^2 c_4^2 c_5 + c_1 c_4 c_5^2 > c_1 c_2^2 c_5^2$.

Since the principal leading diagonal of the Jacobean matrix is all positive, the disease-free equilibrium point E_0 is locally asymptotically stable.

3.6 Global Stability

The following theorem is presented to comprehend the disease-free equilibrium's global stability.

Theorem 3.5. If $\mathcal{R}_0 < 1$, the disease-free equilibrium is globally asymptotically stable, and unstable otherwise.

Proof. Apply the comparison theorem [49] to ascertain global stability while accounting for the derivatives of the diseased compartments in model system (3).

$$\begin{pmatrix} \frac{dE}{dt} \\ \frac{dW}{dt} \\ \frac{dD}{dt} \\ \frac{dM}{dt} \\ \frac{dH}{dt} \end{pmatrix} = (F - V) \begin{pmatrix} E \\ W \\ D \\ M \\ H \end{pmatrix} - \begin{pmatrix} 0 & k_1 \tau_2 & 0 & 0 & \frac{k_1 \tau_1}{d} \\ 0 & 0 & 0 & 0 & 0 \\ 0 & 0 & 0 & 0 & 0 \\ 0 & 0 & 0 & 0 & 0 \\ 0 & 0 & 0 & 0 & 0 \end{pmatrix} \begin{pmatrix} E \\ W \\ D \\ M \\ H \end{pmatrix} \quad (19)$$

$$\begin{pmatrix} \frac{dE}{dt} \\ \frac{dW}{dt} \\ \frac{dD}{dt} \\ \frac{dM}{dt} \\ \frac{dH}{dt} \end{pmatrix} \leq (F - V) \begin{pmatrix} E \\ W \\ D \\ M \\ H \end{pmatrix} \quad (20)$$

The matrices F and V presented in equations (19) and (20) are the following Jacobian matrices:

$$F = \begin{pmatrix} 0 & k_1 \tau_2 & 0 & 0 & \frac{k_1 \tau_1}{d} \\ 0 & 0 & 0 & 0 & 0 \\ 0 & 0 & 0 & 0 & 0 \\ 0 & 0 & 0 & 0 & 0 \\ 0 & 0 & 0 & 0 & 0 \end{pmatrix} \quad (21)$$

and

$$V = \begin{pmatrix} \alpha + \omega & 0 & 0 & 0 & 0 \\ -\omega & \alpha + \rho + \theta & 0 & 0 & 0 \\ 0 & -\theta & \nu & 0 & 0 \\ -\nu & -\gamma & -\pi & \eta & 0 \\ 0 & 0 & 0 & -\eta & \mu \end{pmatrix}. \quad (22)$$

Since the eigenvalues of matrix $(F - V)$ have a negative real part, model (3) is stable at any time $\mathfrak{R}_0 < 1$. Then $(P, E, W, T, D, M, H) \rightarrow (P^0, 0, 0, 0, 0, 0, 0)$ and $P \rightarrow P^0$ as $t \rightarrow \infty$. Considering the comparison theorem, we have $(P, E, W, T, D, M, H) \rightarrow E_0$ as $t \rightarrow \infty$. Therefore, the disease-free equilibrium is globally asymptotically stable.

4 Data Presentation and Parameter Estimation

Ward extension staff, the district agriculture offices, and the Naliendele Agriculture Research Institution in Mtwara participated in the survey for data collection. The maximum likelihood method was used to fit and estimate the model parameters. The data for model fitting was obtained in the Lindi and Mtwara regions specifically.

4.1 Data Presentation

The most crucial components of modelling are model fitting and parameter estimation. After developing a mathematical model and collecting data for the desired class, one is well-positioned to fit the data into the model and determine its parameters [50]. The collected data based on cashew plant death due to *Fusarium* wilt disease came from seven districts in the Lindi and Mtwara regions in Tanzania. The districts where research was conducted included Tandahimba, Masasi, Newala and Mtwara Rural in the Mtwara region, while in the Lindi region, Liwale, Ruangwa and Lindi Rural were involved. The collected data was used in model parameter estimation. A summary of the data is presented in Table 1.

Table 2 Infected dead cashew plants from the year 2018 to 2020.

Village Serial number	Village	Number of disease-induced dead plants	Village serial number	Village	Number of disease-induced dead plants
1	Kitandi	15	15	Kitangali	50
2	Chinongwe	45	16	Chikunja	30
3	Ruhokwe	46	17	Msikisi	16
4	Simana	23	16	Makululu	15
5	Tuungane B	56	19	Mnavila	17
6	Tuungane A	11	20	Makong'on da	41
7	Ungongolo Sokoni	24	21	Lukuledi	48
8	Majimaji	40	22	Mchauru	7
9	Legeza mwendo	15	23	Mpindimbi	9
10	Itete	50	24	Namyomyo	51
11	Dihimba	39	25	Nangoo	190
12	Tandika	31	26	Nanganga	204
13	Mwera Sokoni	13			
14	Nakayaka	33			

Source: Field data 2020

4.2 Estimation of Parameters And Model Fitting

The Matlab program was used to conduct a numerical simulation of model (1). The proposed model's parameter estimation and model fitting were done using maximum likelihood estimation (MLE), as described in [51]. Model fitting is essential since it determines the parameter values for a specific model system based on the data [26]. The initial parameter values, shown in Table 2, were generated from various publications, such as cashew plant carrying capacity k_1 [52], the force of infection between chlamydo spores fungus and susceptible plants τ_1 [53], the force of infection between infected plants and susceptible plants τ_2 [54], the saturation rate of fungus in the soil d [25], progression rate ω [18]. However, we assumed other parameter values based on epidemiological implications.

A graph of the model solution using data and values from the literature against time is shown in Table 1. The high deviation between the model solution and the data shown in Figure 3a indicates the necessity of parameter estimation. In comparison to Figure 3a, Figure 3b displays better results, and the solution of the model with the estimated parameters tends to follow the trend of the data. Table 2 shows the numerical values for each estimated parameter.

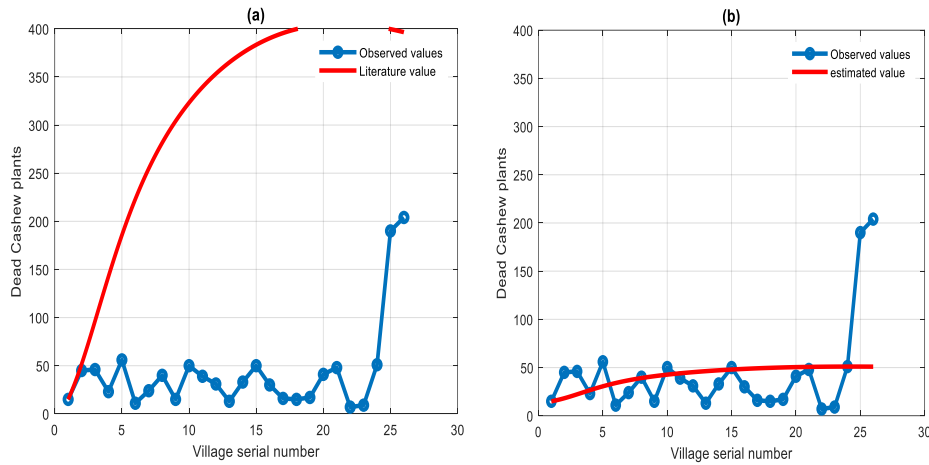


Figure 3 (a) Model solution with values from the literature that seems to diverge from the field data. (b) Fitting of the model solution with estimated values and field data that show convergence.

Table 3 Parameter values estimated and values from the literature.

Parameter	Literature value	Estimated value	Parameter	Literature value	Estimated
r	0.05	0.0605	ρ	0.3	0.3757
k_1	69 hector ⁻¹	74 hector ⁻¹	η	0.5	0.4784
τ_1	0.06	0.0608	μ	0.05	0.0655
τ_2	0.0018	0.0016	ν	0.05	0.0587
d	40 m ⁻² colony site density	45.4016	ϕ	0.3	0.3081
ω	0.5 year	0.4	ν	0.05	0.0481
α	0.005	0.00038	γ	0.2	0.1968
θ	0.8	0.093	π	0.4	0.4125

5 Numerical Analysis

5.1 Local Sensitivity Analysis

This analysis gives indices that help determine how important each parameter is for Fusarium wilt disease transmission and incidence [55]. The local sensitivity analysis examines what happens to \mathfrak{R}_0 when some parameters vary, employing the formula proposed by Arriola and Hyman [56]. Using sensitivity indices, we may evaluate how the state variable has changed relative to a parameter change. The normalized forward sensitivity index of a variable to a parameter measures how much the variable changes with a parameter [57]. The normalized forward sensitivity index is acquired when \mathfrak{R}_0 is differentiable with respect to a given parameter, let's say q , and can be computed as:

$$Y_q^{\mathfrak{R}_0} = \frac{\partial \mathfrak{R}_0}{\partial q} \times \frac{q}{\mathfrak{R}_0}.$$

The result is presented in Figure 4.

The output in Figure 4 indicates that the transmission rate of infection from the soil to vulnerable plants τ_1 and the decomposed disease-induced death rate π strongly influence disease transmission. Furthermore, if the treatment rate ρ and fungus decay rate μ have negative indices, the increase in ρ and μ will decrease disease transmission.

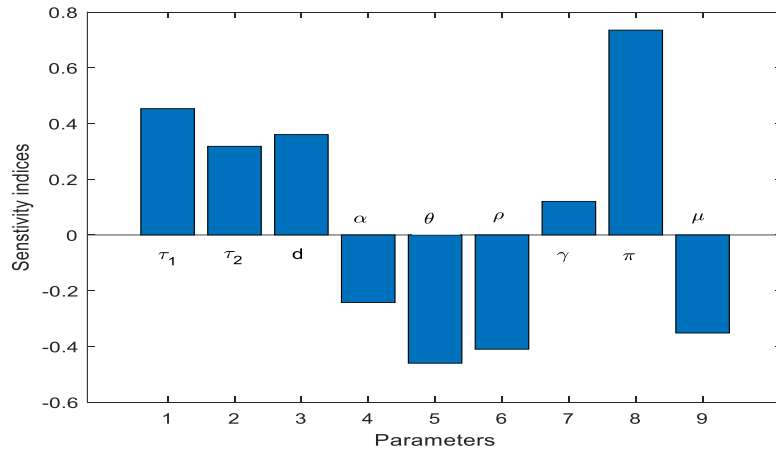


Figure 4 Local sensitivity analysis.

5.2 Global Sensitivity Analysis

The analysis was examined when all parameters were simultaneously varied across the entire range of each parameter. The results of this analysis, which was conducted using the partial rank correlation coefficient (PRCC) method, are shown in Figure 5. The results show that the decomposed disease-induced death rate π and fungus saturation in the soil d increase the transmission of the disease. This means disease transmission increases as the values of the mentioned parameters decrease. Furthermore, disease transmission will decrease when the fungus decay rate μ , the number of dead plants remaining in the field ν , and the disease-induced death rate θ increase.

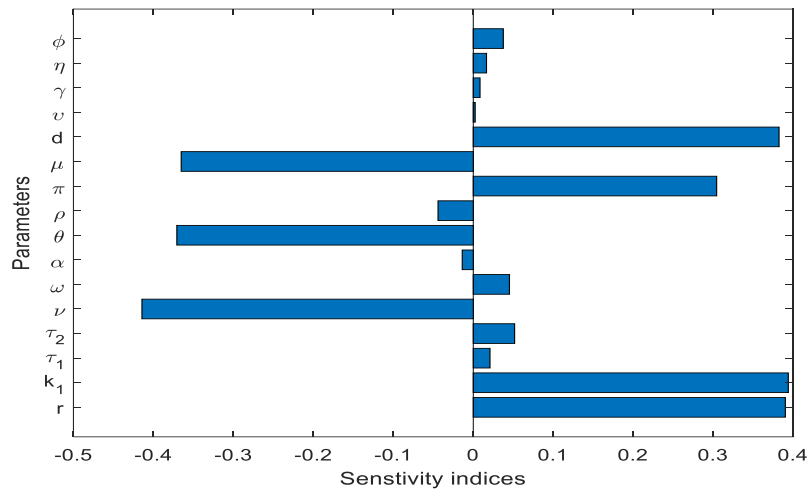
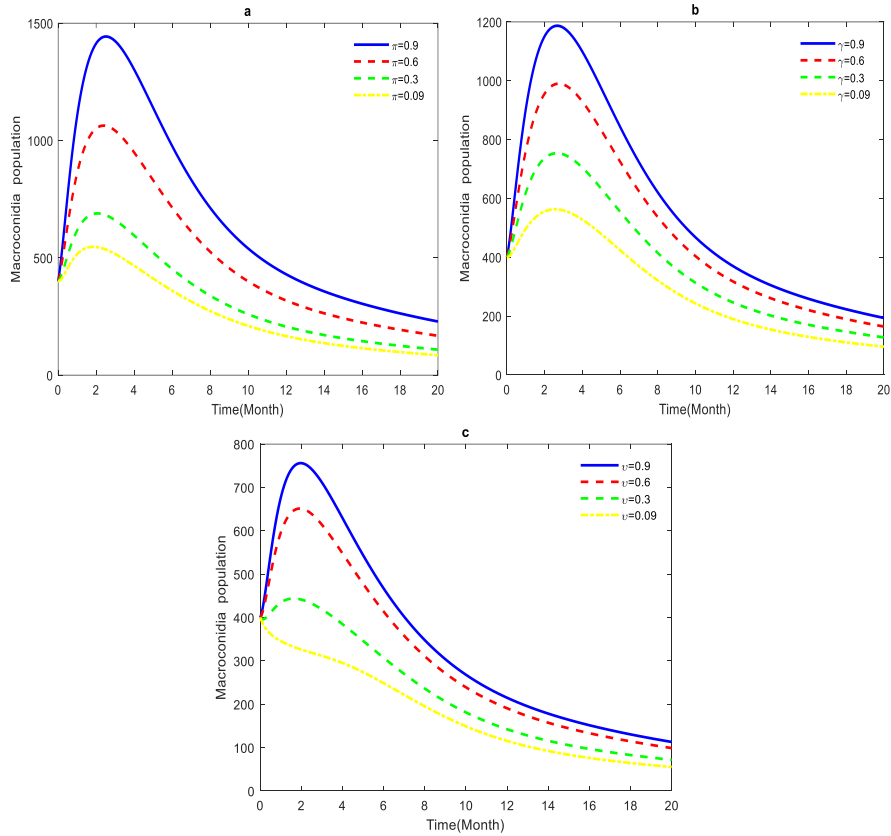


Figure 5 Global sensitivity analysis was conducted using the PRCC technique.

5.3 Effect of Decomposed Disease-Induced Dead Plants on Disease Transmission

Figures 6a, 6b and 6c show the contribution of decomposed disease-induced dead, infected, and exposed dead plants in producing macroconidia. Sporodochia from the dead infected plants produce macroconidia. Macroconidia spores are a saprophytic fungus that plays an important role in decomposition as it performs the initial steps [58],[59]. The growth rate of macroconidia increased in the first four months, as shown in Figures 6 a, b and c, due to the availability of food (dead plants). The growth rate from five to twenty months decreased as the decomposition rate increased. The increase in the macroconidia population led to a rise in disease transmission due to the increase in the chlamydospore population in the soil. Therefore, the presence of dead plants during an outbreak should be considered in planning and selecting a disease control method.



Figures 6 (a) Macroconidia spores population increases due to decomposition of diseased-induced dead plants. (b) Macroconidia spores population increases due to the decay of infected dead plants. (c) Macroconidia spores population increases due to the deterioration of exposed dead plants.

5.4 Effect of Decomposed Disease-Induced Dead Plants on Chlamydo spores Growth

Figure 7 illustrates the impact of chlamydo spore growth in the soil due to an increase of the amount of decomposed disease-induced plants. Decomposed disease-induced plants produce macroconidia spores. Macroconidia spores produce chlamydo spores after the decomposition of dead plants since the environment is not conducive to the survival of macroconidia. Chlamydo spores have thick walls, enabling them to survive in the dry season and increase disease transmission in a conducive environment. Chlamydo spore saturation in the ground causes disease outbreak, which reduces the number of susceptible plants in the field. The number of susceptible plants decreases after the disease progresses to exposed plants. Initially, the number of exposed plants increases up to a certain level before reducing due to the transformation of infected plants. The macroconidia population decreases due to the production of chlamydo spores.

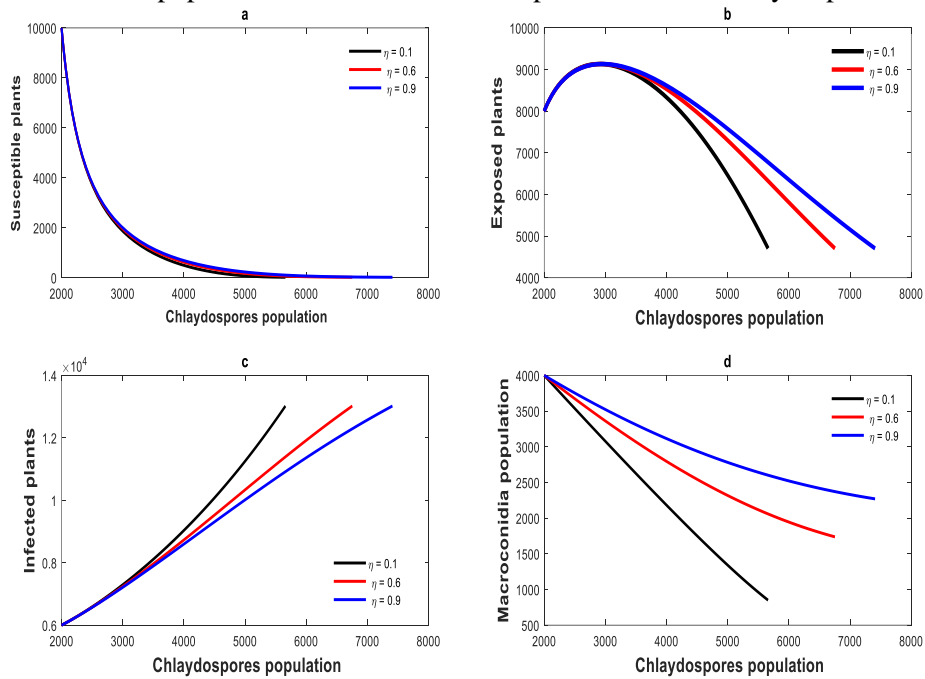


Figure 7 (a) Susceptible plant populations decline as more plants are exposed to the disease. (b) More plants become exposed because the interaction rate increases (c) An infected plants increase due to the rise of chlamydo spores in the ground. (d) An increase in chlamydo spores in the soil leads to a decrease in macroconidia spores.

6 Conclusion

This study addressed the role of decomposed disease-induced dead plants in the spread of cashew *Fusarium* wilt disease. Significant financial losses are caused by the disease, particularly for people or communities that depend on the cashew industry. Sensitivity analysis was conducted to consider the expected uncertainty in parameter values. It was discovered through local and global sensitivity analyses that various factors contribute to the disease's persistence and transmission. A critical factor during outbreaks are decayed disease-induced dead plants. The numerical solution determined the production of macroconidia from decayed disease-induced dead plants that contribute to the production of chlamydospores. The decomposition plays a vital role in ecosystems for nutrient redistribution in the soil. However, since it consists of disease-induced dead plants, this process increases chlamydospore saturation in the ground and hence disease prevalence and spread during an outbreak. Therefore, the presence of decomposed disease-induced dead plants should be considered when developing efficient methods of managing the infection rate during an outbreak.

Reference

- [1] Brufau, G., Boatella, J. & Rafecas, M., *Nuts: Source of Energy and Macronutrients*, Br. J. Nutr., **96**(2), pp. 24-28, 2006. DOI: 10.1017/BJN20061860.
- [2] Dendena, B. & Corsi, S., *Cashew, From Seed to Market: A Review*, Agron. Sustain. Dev., **34**, pp. 753-772, 2014. DOI: 10.1007/s13593-014-0240-7.
- [3] Menge, D.O.M.I.N.I.C. & Shomari, S., *Studies on Leaf and Nut Blight of Cashew (Anacardium Occidentale) Caused by Cryptosporiopsis sp. in Tanzania*, 2016.
- [4] Mukuddem-Petersen, J., Stonehouse, W., Jerling, J.C., Hanekom, S.M. & White, Z., *Effects of A High Walnut and High Cashew Nut Diet on Selected Markers of the Metabolic Syndrome: A Controlled Feeding Trial*, Br. J. Nutr., **97**(6), pp. 1144-1153, 2007. DOI: 10.1017/S0007114507682944.
- [5] Ramadhani, H.A., Kassim, N., Lyimo, B. & Matemu, A., *Physicochemical Quality of Street Vended Roasted Cashew Nuts In Tanzania*, Am. J. Res. Commun., **2**(9), pp. 175-184, 2014. Available: www.usa-journals.com.
- [6] Nene, W. & Sijaona, M., *Assessment of Incidences And Severity of Cashew Leaf and Nut Blight Disease (CLNBD) in the Southern Areas of Tanzania*, Int. J. Sci. Res., **6**(10), pp. 1589-1594, 2017.
- [7] Wonni, I., Sereme, D., Ouédraogo, I., Kassankagno, A.I., Dao, I., Ouedraogo, L. & Nacro, S., *Diseases of Cashew Nut Plants (Anacardium occidentale L.) in Burkina Faso*, Adv. Plants Agric. Res., **6**(3), 00216,

2017. DOI: 10.15406/apar.2017.06.00216.
- [8] Majune, D., Masawe, P. & Mbega, E., *Status and Management of Cashew Disease in Tanzania*, Int. J. Environ. Agric. Biotechnol., **3**(5), pp. 1590-1597, 2018. DOI: 10.22161/ijeab/3.5.4.
 - [9] Sijaona, M.E.R., Reeder, R.H. & Waller, J.M., *Cashew Leaf and Nut Blight – A New Disease of Cashew In Tanzania Caused by Cryptosporiopsis sp.* Plant Pathology, **55**(4), 55576, 2006.
 - [10] Ellis, F., *A Preliminary Analysis of the Decline in Cashew Nut Production, 1974-1979: Causes, Possible Remedies and Lessons for Rural Development Policy*, Dar es salaam, 1980.
 - [11] Brown, L.C., Minja, E. & Hamad, A.S., *Cashew Production in East Africa. Paper Presented at CABI's First Scientific Conference on Advancing Agricultural Production in Africa*, in Proceedings of CAB's 1st. Scientific Conference Arusha, pp. 160-163, 1984.
 - [12] Tibuhwa, D.D. & Shomari, S., *Fusarium Wilt Disease: An Emerging Threat to Cashew Nut Crop Production in Tanzania.*, Asian J. Plant Pathol. Pathol., **10**, pp. 36-48, 2016.
 - [13] Okungbowa, F.I. & Shittu, H.O., *Fusarium Wilts: An Overview*, Environ. Res. J., **6**(2), pp. 83–102, 2016.
 - [14] Moore, N.Y., Bentley, S., Pegg, K.G. & Jones, D.R.J., *Musa Disease Fact Sheet N° 5 Fusarium Wilt of Banana*, in International Network for the Improvement of Banana and Plantain, Parc Scientifique Agropolis (Inibap), 1995.
 - [15] Mbasa, W.V., Nene, W.A., Kapinga, F.A., Lilai, S.A. & Tibuhwa, D.D., *Characterization and Chemical Management of Cashew Fusarium Wilt Disease Caused by Fusarium Oxysporum in Tanzania*, Crop Prot., **139**, 105379, 2021. DOI: 10.1016/j.cropro.2020.105379.
 - [16] Punja, Z.K. & Parker, M., *Development of Fusarium Root and Stem Rot, A New Disease on Greenhouse Cucumber in British Columbia, Caused by Fusarium oxysporum f. sp. radicis-cucumerinum*, Can. J. Plant Pathol., **22**(4), pp. 349-363, 2000. DOI: 10.1080/07060660009500453.
 - [17] Flood, J., *Fusarium – A Review of Fusarium wilt of oil palm caused by Fusarium oxysporum f. sp. elaeidis*, Phytopathology, **96**(6), pp. 660-662, 2006.
 - [18] Pegg, K.G., Coates, L.M., O'Neill, W.T. & Turner, D.W., *The Epidemiology of Fusarium Wilt of Banana*, Front. Plant Sci., **10**, pp. 1-19, 2019. DOI: 10.3389/fpls.2019.01395.
 - [19] Hohle, M., *Infectious Disease Modelling*, Handb. Spat. Epidemiol., pp. 477-500, 2015.
 - [20] Kumar, S., Kumar, R., Osman, M.S. & Samet, B., *A Wavelet Based Numerical Scheme for Fractional Order SEIR Epidemic of Measles by Using Genocchi Polynomials*, Numer. Methods Partial Differ. Equ., **37**(2), pp. 1250–1268, 2021. DOI: 10.1002/num.22577.

- [21] Khan, M.A., Ullah, S. & Kumar, S., *A Robust Study On 2019-Ncov Outbreaks Through Non-Singular Derivative*, Eur. Phys. J. Plus, **136**, pp. 1-20, 2021. DOI: 10.1140/epjp/s13360-021-01159-8.
- [22] Mohammadi, H., Kumar, S., Rezapour, S. & Etemad, S., *A Theoretical Study of the Caputo–Fabrizio Fractional Modelling For Hearing Loss due to Mumps Virus with Optimal Control*, Chaos, Solitons and Fractals, **144**, 110668, 2021. DOI: 10.1016/j.chaos.2021.110668.
- [23] Kumar, S., Chauhan, R.P., Momani, S. & Hadid, S., *Numerical Investigations on COVID-19 Model through Singular and Non-Singular Fractional Operators*, Numer. Methods Partial Differ. Equ., pp. 1-27, 2020. DOI: 10.1002/num.22707.
- [24] Kumar, S., Kumar, A., Samet, B. & Dutta, H., *A Study on Fractional Host–Parasitoid Population Dynamical Model to Describe Insect Species*, Numer. Methods Partial Differ. Equ., **37**(2), pp. 1673-1692, 2021. DOI: 10.1002/num.22603.
- [25] Burie, J.B., Calonnec, A. & Langlais, M., *Modelling of the Invasion of A Fungal Disease Over A Vineyard*, in Mathematical Modeling of Biological Systems, Volume II: Epidemiology, Evolution and Ecology, Immunology, Neural Systems and the Brain, and Innovative Mathematical Methods, pp. 11–21, 2008.
- [26] Anggriani, N., Putri, L.N. & Supriatna, A.K., *Stability Analysis and Optimal Control of Plant Fungal Epidemic: An Explicit Model with Curative Factor*, Symp. Biomath. (SYMOMATH 2014), **1651**(1), pp. 40-47, 2015.
- [27] Nisar, K.S., Logeswari, K., Vijayaraj, V., Baskonus, H.M. & Ravichandran, C., *Fractional Order Modeling the Gemini Virus in Capsicum annuum with Optimal Control*, Fractal Fract., **6**(2), pp. 1-19, 2022. DOI: 10.3390/fractalfract6020061.
- [28] Anggriani, N., Mardiyah, M., Istifadah, N. & Supriatna, A.K., *Optimal Control Issues in Plant Disease with Host Demographic Factor and Botanical Fungicides*, in IOP Conference Series: Materials Science and Engineering, **332**(1), 012036, 2018.
- [29] Khan, M.A., Ali, K., Bonyah, E., Okosun, K.O., Islam, S. & Khan, A., *Mathematical Modelling and Stability Analysis of Pine Wilt Disease with Optimal Control*, Sci. Rep., **7**(1), pp. 1-19, 2017.
- [30] Murwayi, A., Onyango, T. & Owour, B., *Mathematical Analysis of Plant Disease Dispersion Model that Incorporates Wind Strength and Insect Vector at Equilibrium*, Br. J. Math. Comput. Sci., **22**(5), pp. 1-17, 2017. DOI: 10.9734/BJMCS/2017/33991.
- [31] Sajjad, A., Farman, M., Hasan, A. & Nisar, K.S., *Transmission Dynamics of Fractional Order Yellow Virus in Red Chili Plants with the Caputo–Fabrizio Operator*, Math. Comput. Simul., **207**, pp. 347-368, 2023. DOI:

- 10.1016/j.matcom.2023.01.004.
- [32] Hussain, T., Ozair, M., Faizan, M., Jameel, S. & Nisar, K.S., *Optimal Control Approach Based on Sensitivity Analysis to Retrench the Pine Wilt Disease*, Eur. Phys. J. Plus, **136**(7), pp. 1-27, 2021. DOI: 10.1140/epjp/s13360-021-01695-3.
 - [33] Daly, A.M. & Walduck, G., *Fusarium Wilt of Bananas (Panama Disease) (Fusarium oxysporum f. sp. cubense)*, 2006.
 - [34] Inoue, I., Namiki, F. & Tsuge, T., *Plant Colonization by the Vascular Wilt Fungus Fusarium oxysporum Requires FOW1, A Gene Encoding A Mitochondrial Protein*, The Plant Cell, **14**(8), pp. 1869-1883, 2002.
 - [35] Pérez-Vicente, L., Dita, M.A., & Martínez-de la Parte, E., *Technical Manual: Prevention and Diagnostic of Fusarium Wilt (Panama Disease) of Banana Caused by Fusarium oxysporum f. sp. Cubense. Tropical Race 4 (TR4)*. Prevention and Diagnostic of Fusarium Wilt (Panama Disease) of Banana Caused by Fusarium oxysporum f. sp. Cubense. Tropical Race 4 (TR4), in Workshop on Diagnosis of Fusarium Wilt, 2014, **4**, pp. 1-74, 2015.
 - [36] Rana, A., Sahgal, M. & Johri, B.N., *Fusarium oxysporum: Genomics, Diversity and Plant–Host Interaction*, in Developments in Fungal Biology and Applied Mycology, pp. 159-199, 2017.
 - [37] Pietro, A.D., Madrid, M.P., Caracuel, Z., Delgado-Jarana, J. & Roncero, M. I., *Fusarium oxysporum: Exploring the Molecular Arsenal of A Vascular Wilt Fungus*, Mol. Plant Pathol., **4**(5), pp. 315-325, 2003. DOI: 10.1046/J.1364-3703.2003.00180.X.
 - [38] Ohara, T. & Tsuge, T., *FoSTUA, Encoding A Basic Helix-Loop-Helix Protein, Differentially Regulates Development of Three Kinds of Asexual Spores, Macroconidia, Microconidia, and Chlamydospores, in the Fungal Plant Pathogen Fusarium oxysporum*, Eukaryot. Cell, **3**(6), pp. 1412-1422, 2004. DOI: 10.1128/EC.3.6.1412.
 - [39] Ohara, T., Inoue, I., Namiki, F., Kunoh, H. & Tsuge, T., *REN1 is Required for Development of Microconidia and Macroconidia, but Not of Chlamydospores, in the Plant Pathogenic Fungus Fusarium oxysporum*, J. Genet., **166**(1), pp. 113-124, 2004.
 - [40] Madden, L.V., *Effects of Rain on Splash Dispersal of Fungal Pathogens*, Can. J. Plant Pathol., **19**(2), pp. 225-230, 1997. DOI: 10.1080/07060669709500557.
 - [41] Inch, S., Fernando, W.G.D. & Gilbert, J., *Seasonal and Daily Variation in the Airborne Concentration of Gibberella zeae (Schw.) Petch Spores in Manitoba*, Can. J. Plant Pathol., **27**(3), pp. 357-363, 2005. DOI: 10.1080/07060660509507233.
 - [42] Fernando, W.G., Miller, J.D., Seaman, W.L., Seifert, K. & Paulitz, T.C., *Daily and Seasonal Dynamics of Airborne Spores of Fusarium graminearum and ther Fusarium Species Sampled over Wheat Plots*, Can.

- J. Bot., **78**(4), pp. 497-505, 2000. DOI: 10.1139/cjb-78-4-497.
- [43] Dutta, B., Searcy, J. & Coolong, T., *Fusarium Wilt of Watermelon*, UGA Coop, Ext. Bull, 2017.
 - [44] Ma, L.J., Geiser, D.M., Proctor, R.H., Rooney, A.P., O'Donnell, K., et al., *Fusarium Pathogenomics*, **67**, pp. 399-416, 2013. DOI: 10.1146/annurev-micro-092412-155650.
 - [45] Kang, S., Demers, J., del Mar Jimenez-Gasco, M. & Rep, M., *Fusarium oxysporum*, Genomics of Plant-Associated Fungi and Oomycetes: Dicot Pathogens, pp. 99-119, 2014.
 - [46] Schwartz, H.F., Gent, D.H., Franc, G.D. & Harveson, R.M., *Fusarium Wilt*, Dry Bean Production & Pest Management. Coop. Ext. Reg. Bull. A, **562**, 115, 2004.
 - [47] Van den Driessche, P. & Watmough, J., *Reproduction Numbers and Sub-threshold Endemic Equilibria for Compartmental Models of Disease Transmission*, Math. Biosci., **180**(1-2), pp. 29-48, 2002. DOI: 10.1016/S0025-5564(02)00108-6.
 - [48] Choghadi, M.A. & Talebi, H.A., *The Routh-Hurwitz Stability Criterion, Revisited: The Case of Multiple Poles on Imaginary Axis*, IEEE Trans. Automat. Contr., **58**(7), pp. 1866-1869, 2013.
 - [49] Shaban, N., *Modelling the Effects of Public Health Education in the Spread of Hepatitis B Disease*, Appl. Math. Sci., **9**(80), pp. 3967-3981, 2015. DOI 10.12988/ams.2015.44289.
 - [50] Myung, I.J., *Tutorial on Maximum Likelihood Estimation*, J. Math. Psychol., **47**(1), pp. 90-100, 2003. DOI: 10.1016/S0022-2496(02)00028-7.
 - [51] Pan, J.X. & Fang, K.T., *Growth Curve Models and Statistical Diagnostics*, Beijing: Springer Science and Business Media New York, 2002.
 - [52] Martin, P.J., Topper, C.P., Bashiru, R.A., Boma, F.D., De Waal, D., et al., *Cashew Nut Production in Tanzania: Constraints and Progress through Integrated Crop Management*, Crop Prot., **16**(1), pp. 5-14, 1997. DOI: 10.1016/S0261-2194(96)00067-1.
 - [53] Chan, M.S. & Jeger, M.J., *An Analytical Model of Plant Virus Disease Dynamics with Roguing and Replanting*, J. Appl. Ecol., **31**(3), pp. 413-427, 1994. DOI: 10.2307/2404439.
 - [54] Collins, O.C. & Duffy, K.J., *Optimal Control of Maize Foliar Diseases using the Plants Population Dynamics*, Acta Agric. Scand., Section B-Soil & Plant Science, **66**(1), pp. 20-26, 2016. DOI: 10.1080/09064710.2015.1061588.
 - [55] Chitnis, N., Hyman, J.M. & Cushing, J.M., *Determining Important Parameters in the Spread of Malaria through the Sensitivity Analysis of A Mathematical Model*, Bull. Math. Biol., **70**, pp. 1272-1296, 2008. DOI: 10.1007/s11538-008-9299-0.

- [56] Arriola, L. & Hyman, J.M., *Sensitivity Analysis for Uncertainty Quantification in Mathematical Models*, In Mathematical and statistical estimation approaches in epidemiology, pp. 195-247, 2009.
- [57] Phaijoo, G.R. & Gurung, D.B., *Sensitivity Analysis of {SEIR-SEI} Model of Dengue Disease*, GAMS J. Math. Math. Biosci., **6**, pp. 41-50, 2018.
- [58] Francioli, D., van Rijssel, S.Q., van Ruijven, J., Termorshuizen, A.J., Cotton, T.A., et al., *Plant Functional Group Drives the Community Structure of Saprophytic Fungi in A Grassland Biodiversity Experiment*, Plant and Soil, **461**(1–2), pp. 91-105, 2021. DOI: 10.1007/s11104-020-04454-y.
- [59] Crowther, T.W., Boddy, L. & T Jones, H., *Functional and Ecological Consequences of Saprotrophic Fungus-Grazer Interactions*, The ISME J., **6**(11), pp. 1992-2001, 2012. DOI: 10.1038/ismej.2012.53.